

Solubility of fluorinated compounds in a range of ionic liquids. Cloud-point temperature dependence on composition and pressure

Rui Ferreira,^a Marijana Blesic,^a Joana Trindade,^a Isabel Marrucho,^b José N. Canongia Lopes^{*a,c} and Luís Paulo N. Rebelo^{*a}

Received 8th April 2008, Accepted 17th June 2008

First published as an Advance Article on the web 11th August 2008

DOI: 10.1039/b805902k

In this work, we explore the mutual solubility of a number of mixtures of commonly used ionic liquids (imidazolium, pyridinium, phosphonium and ammonium ionic liquids) with partially fluorinated *n*-alcohols (C₇ to C₁₀) or perfluoroheptane. The corresponding *T*-*x* diagrams at atmospheric pressure were measured through cloud-point temperature determinations. For some selected systems under near-critical isopleth conditions, pressure effects were also studied. The results are discussed in terms of (i) shifts in the immiscibility envelopes as the cation alkyl-chain length is changed, (ii) the nature of the cation or the anion, (iii) the increasing length of the fluorinated/alkylic moiety of the partially fluorinated alcohol, or (iv) comparisons with similar systems involving normal alcohols.

1. Introduction

One of the key-issues concerning the current importance of ionic liquids is the fact that they can simultaneously act as sophisticated solvation or reaction media while avoiding dramatic impacts in the environment due to their general low volatility and flammability combined with high thermal stability. Ionic liquids are able to dissolve (at least partially) a wide range of polar or nonpolar, organic or inorganic compounds,¹ providing new ways to carry out chemical reactions or industrial separations.²

It was recently reported in different molecular simulation studies³ that neat ionic liquids exhibit medium-range ordering, in other words, there are persistent microscopic domains in the liquid phase. Other simulation studies⁴ on the microscopic dynamics of ionic liquids have also pointed out their slow dynamics and the persistence of local environments, typical of the glassy state.

The segregation in polar and nonpolar domains at a nano-scale level in ionic liquids with alkyl side chains of intermediate length (for instance in 3-alkyl-1-methylimidazolium-based ionic liquids with alkyl groups larger than hexyl), has changed the way in which solvation in these liquids is understood. Some solutes dissolve preferentially in low electrical charge-density domains, while others prefer the Coulomb environment of high electrical-charge density regions, whereas some can even “be dissolved” at the interface between these polar and non-polar territories.⁵ These facts account for the extraordinary versatility of ionic liquids as solvents.

Fluorinated organic compounds also display many exceptional physico-chemical properties that have been used in many commercial applications. Similar to ionic liquids, they are also perceived as alternative substances towards the development of

more environmentally friendly processes. Industrial production of these compounds has increased significantly since the early 1980s and fluorinated organics are commonly used as refrigerants, surfactants, polymers, as components of pharmaceuticals, fire retardants, lubricants, and insecticides.⁶ In recent years the possibility of their use as gas-carriers (including the possibility of their use as synthetic blood substitutes),⁷ and as solubility-promoters in supercritical extraction media⁸ has also been explored. From a molecular point of view, the properties of fluorinated organic compounds can be rationalized in terms of the unique interactions they perform with different molecules: fluorocarbons generally exhibit low-intensity interactions with normal organic compounds⁹ or water, a fact related not only to their “reversed” quadrupole moment (note that the carbon backbone of a perfluorocarbon molecule carries a partially positive charge, due to the high electronegativity of the fluorine atom, unlike the situation in hydrocarbons or water) but also due to their relatively rigid structure (that inhibits the existence of different conformers and introduces entropic-driven factors in mixtures with other substances).

Functionalized fluorocarbons were also studied in recent years due to their amphiphilic behaviour and their possible use as separation media or surfactant agents. Examples of such compounds are the hydrofluorocarbon molecules,¹⁰ the hydrocarbon-fluorocarbon diblock molecules¹¹ and the fluorinated alcohols.¹² The rationale behind the synthesis and use of such molecules is the introduction of an interacting group in the otherwise inert perfluorinated chain, that will promote the “docking” of the fluorinated compound in the midst of other molecules (with the possible self-organization of the former in micelles or similar structures) or the formation of emulsions between fluorinated and organic or aqueous domains.

Systems where both types of compound, ionic liquids and fluorinated organic molecules, are inherently appealing as they are perceived as relatively benign media, combining two “clean” substances. This blend also poses very interesting challenges both from the theoretical and the applied chemistry points of

^aInstituto de Tecnologia Química e Biológica, UNL, 2780 901, Oeiras, Portugal. E-mail: luis.rebelo@itqb.unl.pt

^bCICECO, Universidade de Aveiro, 3810 193, Aveiro, Portugal

^cCentro de Química Estrutural, IST, 1049 001, Lisboa, Portugal. E-mail: jnlopes@ist.utl.pt

view. As an example of the former aspect, one can hope to gain some insight about the interactions between the fluorinated molecules and the parts of the ionic liquid that are themselves fluorinated (generally present in anions such as bistriflamide, triflate or hexafluorophosphate). An example of the latter issue can be, for instance, the possibility of using partially fluorinated alcohols or diblock molecules to promote the miscibility (through the formation of micro-emulsions) between bistriflamide-based ionic liquids and aqueous solutions.

In this work, we explore the fluid phase diagrams of mixtures of commonly used ionic liquids with partially fluorinated alcohols. The systems are analyzed in terms of the two-phase envelopes (immiscibility regions) of the corresponding $T-x$ diagrams at atmospheric pressure, which in turn have been determined by the measurement of cloud-point temperatures as a function of the mixture compositions. Pressure effects were also studied for some selected systems under near-critical isopleth conditions. The results are discussed in terms of shifts in those envelopes as the alkyl side chains of the cations get longer, the nature of the cation or the anion is changed, the length of the fluorinated moiety of the partially fluorinated alcohol is increased, or by comparison with systems involving normal alcohols (ethanol and propanol). We have also noticed the essentially total immiscible behaviour of a range of ionic liquids studied in this work with a linear perfluorinated alkane.

2. Experimental

Materials

Table 1 shows the compounds involved in the detailed determination of the fluid phase behaviour of mixtures of ionic liquids with fluorinated alcohols. In addition to the compounds listed in Table 1, other ionic liquids and other fluorinated alcohols were used in preliminary solubility tests (see Table 2). The complete list, including name and/or commercial name (abbreviated name; CAS number, source and grade if available), is as follows: 1-ethyl-3-methylimidazolium ethylsulfate, ECOENGTM 212 ($C_2mimEtSO_4$; 342573-75-5; Solvent Innovation; >99%); trioctylmethylammonium chloride, ALIQUATTM 336 ($N_{888}Cl$; 63393-96-4; Aldrich; n/a); trihexyl-(tetradecyl)phosphonium chloride ($P_{66614}Cl$; 258864-54-9; Cytec; >96%); trihexyl(tetradecyl)phosphonium bis[(trifluoromethyl)sulfonyl]imide ($P_{66614}NTf_2$; 460092-03-9; QUILL†; n/a); trihexyl(tetradecyl)-phosphonium trifluoromethanesulfonate ($P_{66614}OTf$; CAS number; QUILL†; n/a); trihexyl(tetradecyl)-phosphonium acetate ($P_{66614}Ac$; 460092-04-0; QUILL†; n/a); 1-ethyl-3-methylimidazolium bis[(trifluoromethyl)sulfonyl]imide ($C_2mimNTf_2$; 174899-82-2; QUILL†; n/a); 1-propyl-3-methylimidazolium bis[(trifluoromethyl)sulfonyl]imide ($C_3mimNTf_2$; 216299-72-8; QUILL†; n/a); 1-pentyl-3-methylimidazolium bis[(trifluoromethyl)sulfonyl]imide ($C_5mimNTf_2$; 280779-53-5; QUILL†; n/a); 1-octyl-3-methylimidazolium bis[(trifluoromethyl)sulfonyl]imide ($C_8mimNTf_2$; 178631-04-4; QUILL†; n/a); 1-decyl-3-methylimidazolium bis[(trifluoromethyl)sulfonyl]imide ($C_{10}mimNTf_2$; 433337-23-6; QUILL†; n/a); 1-dodecyl-3-methylimidazolium bis-

[(trifluoromethyl)sulfonyl]imide ($C_{12}mimNTf_2$; unknown CAS; QUILL†; n/a); acetyl-cholinium bis[(trifluoromethyl)sulfonyl]imide ($AcChNTf_2$; unknown CAS; QUILL†; n/a); 1-hexyl-3-methylimidazolium chloride (C_6mimCl ; 171058-17-6; QUILL#; n/a); 1-dodecyl-3-methylimidazolium chloride ($C_{12}mimCl$; 114569-84-5; QUILL†; n/a); 1-butyl-3-methylimidazolium hexafluoroborate (C_4mimBF_4 ; 174501-65-6; Solvent Innovation GmbH; >99%); 1-butyl-3-methylimidazolium hexafluorophosphate (C_4mimPF_6 ; 174501-64-5; QUILL#; n/a); 1-octyl-3-methylimidazolium hexafluorophosphate (C_8mimPF_6 ; 304680-36-2; QUILL†; n/a); 1-decyl-3-methylpyridinium bis[(trifluoromethyl)sulfonyl]imide ($C_{10}MePyNTf_2$; unknown CAS; QUILL†; n/a); 1-dodecyl-3-methylpyridinium bis[(trifluoromethyl)sulfonyl]imide ($C_{12}MePyNTf_2$; unknown CAS; QUILL†; n/a); 1-tetradecyl-3-methylpyridinium bis[(trifluoromethyl)sulfonyl]imide ($C_{14}MePyNTf_2$; unknown CAS; QUILL†; n/a); 1-tetradecyl-3-methylpyridinium bromide ($C_{14}MePyBr$; unknown CAS; QUILL†; n/a); 1-butyl-3-methylimidazolium thiocyanate ($C_4mimSCN$; 344790-87-0; Fluka; >95%) e 1-butyl-3-methylimidazolium methylsulfate ($C_4mimMeSO_4$; 401788-98-5; Fluka; >97%).

All ionic liquids used in solubility tests were used without any further purification. Ionic liquids used in cloud-point data measurements were previously dried and degassed under vacuum conditions (1 to 10 Pa) at moderate temperatures (80–100 °C) for periods longer than 24 hours.

The list of alcohols used is as follows: ethanol (64-17-5; Pronalab; 99.8%); 1-propanol (71-23-8; Aldrich; 99.7%); 1*H*,1*H*,7*H*-perfluoroheptanol (117-C₇FOH; 335-99-9; Apollo Scientific; 98%); 1*H*,1*H*,2*H*,2*H*-perfluorooctanol (1122-C₈FOH; 647-42-7; ABCR; 98%); 1*H*,1*H*-perfluorooctanol (11-C₈FOH; 307-30-2; Apollo Scientific; 98%); 1*H*,1*H*-perfluorononanol (11-C₉FOH; 423-56-3; Apollo Scientific; 98%); 1*H*,1*H*-perfluorodecanol (11-C₁₀FOH; 307-37-9; Apollo Scientific; 98%); 1*H*,1*H*,2*H*,2*H*,3*H*,3*H*-perfluorononanol (112233-C₉FOH; 80806-68-4; Fluorochem; 98%) and perfluoroheptane (C₇F₁₆; 335-57-9; Apollo Scientific, 98%). All fluorinated alcohols were used without further purification.

Preliminary solubility tests

Solubility tests were performed by adding small amounts (*ca.* 100 μL) of IL and fluorinated compound into a glass (Pyrex) conical vessel containing a magnetic stirrer. Any phase separation (if present) was visually detected. Different composition ranges were tested at temperatures from *ca.* –10 °C up to 70 °C.

Cloud-point measurements

All cloud-point determinations on the temperature–composition phase diagrams of the ionic liquid plus fluorinated alcohol systems at a nominal pressure of 0.1 MPa were performed using a dynamic method with visual detection of the solution turbidity. For this purpose, Pyrex glass view cells with magnetic stirring were used. Samples were gravimetrically prepared directly inside the cells using an analytical high precision balance (±0.01 mg). The cells were then immersed in a thermostatic bath. Providing continuous stirring, we cooled off or heated the solutions usually in two or three runs with the two last runs being carried out very slowly (the

† Queen's University Ionic Liquids Laboratories.

Table 1 Description of the ionic liquids and fluorinated alcohols used in the cloud-point determinations

Formal Name	Structure	Abbreviation
1-Alkyl-3-methylimidazolium bis(trifluoromethylsulfonyl)imide (alkyl = octyl, decyl and dodecyl)		$C_8mimNTf_2$ $C_{10}mimNTf_2$ $C_{12}mimNTf_2$
Acetylcholinium bis(trifluoromethylsulfonyl)imide		$AcChNTf_2$
Trihexyltetradecylphosphonium bis(trifluoromethylsulfonyl)imide		$P_{66614}NTf_2$
1-Alkyl-3-methylpyridinium bis(trifluoromethylsulfonyl)imide (alkyl = decyl, dodecyl and tetradecyl)		$C_{10}MePyNTf_2$ $C_{12}MePyNTf_2$ $C_{14}MePyNTf_2$
1-Octyl-3-methylimidazolium hexafluorophosphate		C_8mimPF_6
1-Butyl-3-methylimidazolium tetrafluoroborate		C_4mimBF_4
1 <i>H</i> ,1 <i>H</i> ,2 <i>H</i> ,2 <i>H</i> -Perfluorooctanol ($n = 2$) 1 <i>H</i> ,1 <i>H</i> ,2 <i>H</i> ,2 <i>H</i> ,3 <i>H</i> ,3 <i>H</i> -Perfluorononanol ($n = 3$)		1122- C_8 FOH 112233- C_9 FOH

rate of temperature change near the cloud point was no more than 5 K h^{-1}). Beginning in the homogeneous region, upon cooling, the temperature at which the first sign of turbidity appeared was taken as the temperature of the liquid–liquid phase transition. Temperature was monitored using a four-wire platinum resistance thermometer coupled to a Yokogawa 7561 multimeter. The thermometer was calibrated against high accuracy mercury thermometers (0.01 K precision). The overall accuracy in the determination of the cloud-point temperatures is estimated to be $\pm 0.3 \text{ K}$.

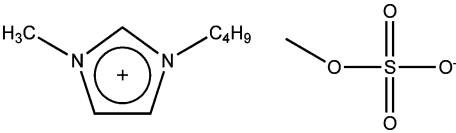
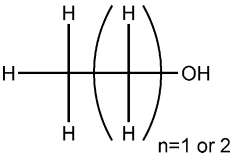
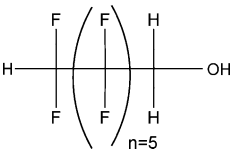
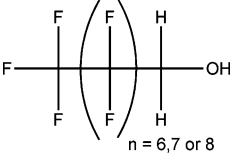
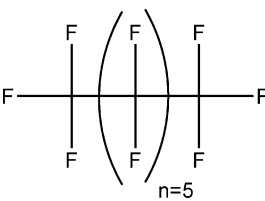
Pressure effects on the cloud-point temperature were obtained by a He–Ne laser light scattering technique. The apparatus and

the methodology used for the determination of phase transitions have already been described in detail.¹³ Here, only a brief description is provided. The cell (with an internal volume of *ca.* 1.0 cm^3 and an optical length of *ca.* 2.6 mm) is a thick-walled Pyrex glass tube that is connected to a pressurization line and separated from it by a mercury plug. The intensity of the scattered light is captured at a very low angle ($2^\circ < 2\theta < 4^\circ$) in the outer portion of a bifurcated optical cable, whereas transmitted light is captured in the inner portion of this cable. The intensity of scattered light (I_{sc}) and transmitted light (I_{tr}) are corrected for density fluctuations, reflections, and multiple scattering effects. The cloud-point is the point on the

Table 2 Description of other compounds, not listed in Table 1, which were used in preliminary solubility tests

Formal Name	Structure	Abbreviation
1-Ethyl-3-methylimidazolium ethylsulfate (ECOENG™ 212)		$C_2mimEtSO_4$
Trioctylmethylammonium chloride (ALIQAT™ 336)		$N_{8881}Cl$
Trihexyl(tetradecyl)phosphonium chloride		$P_{66614}Cl$
Trihexyl(tetradecyl)phosphonium trifluoromethanesulfonate		$P_{66614}OTf$
Trihexyl(tetradecyl)phosphonium acetate		$P_{66614}Ac$
1-Alkyl-3-methylimidazolium bis-[(trifluoromethyl)sulfonyl]imide (alkyl = ethyl, propyl and pentyl)		$C_2mimNTf_2$ $C_3mimNTf_2$ $C_5mimNTf_2$
1-Alkyl-3-methylimidazolium chloride (alkyl = hexyl, dodecyl)		C_6mimCl $C_{12}mimCl$
1-Butyl-3-methylimidazolium hexafluorophosphate		C_4mimPF_6
1-Tetradecyl-3-methylpyridinium bromide		$C_{14}MePyBr$
1-Butyl-3-methylimidazolium thiocyanate		$C_4mimSCN$

Table 2 (Contd.)

Formal Name	Structure	Abbreviation
1-Butyl-3-methylimidazolium methylsulfate		$C_4mimMeSO_4$
Ethanol ($n = 1$) Propanol ($n = 2$)		C_2H_5OH C_3H_7OH
1H,1H,7H-dodecafluoroheptanol		117- C_7FOH
1-(Perfluoroheptyl)methanol ($n = 6$) 1-(Perfluorooctyl)methanol ($n = 7$) 1-(Perfluorononanol)methanol ($n = 8$)		11- C_8FOH 11- C_9FOH 11- $C_{10}FOH$
Perfluoroheptane		C_7F_{16}

least-squares fits of $(I_{sc,corr})^{-1}$ against pressure (p) or temperature (T) where the slope changes abruptly. Temperature accuracy is typically ± 0.01 K in the range $240 \text{ K} < T < 380 \text{ K}$. As for pressure, accuracy is ± 0.01 MPa in the range $0.1 \text{ MPa} < p < 5 \text{ MPa}$. The cell can be operated in the isobaric or isothermal mode. Whenever possible, isothermal runs are preferred over isobaric ones. Pressure transmission (isothermal mode) is many orders of magnitude faster than thermal equilibration (isobaric mode). Also, the rate at which one is able to change pressure is much greater than that for temperature. Nonetheless, many runs had to be performed in the isobaric mode due to the common low T - p slope presented by the binary mixtures being studied here.

3. Results and discussion

The preliminary solubility tests are given in Table 3. These results were used to select the systems that would be more promising in terms of a richer fluid phase behaviour, *i.e.*, systems exhibiting liquid–liquid partial immiscibility (LLE) ending at an upper critical solution temperature, UCST, as

the temperature is increased. For systems presenting this type of phase diagrams one can easily switch between one-phase and two-phase situations either by composition or temperature change. It is important to note that not all systems exhibiting LLE behaviour were selected for the subsequent cloud-point measurements (those that were selected are highlighted in grey in Table 3). There were different types of reasons for the rejection of some of the systems: some systems contained ionic liquids with rather high melting points (an LLE line interrupted by a solid–liquid equilibrium (SLE) line), which can cause problems in terms of turbidity detection; others exhibited degradation problems at temperatures near the UCST; *etc.* The solubility tests were also used to select the “best” fluorinated alcohol—that presenting LLE behaviour in mixtures with different ionic liquids at experimentally convenient conditions. In this case, it was found that a higher number of hydrogenated carbon atoms near the hydroxyl function decreased the miscibility between the ionic liquids and the fluorinated alcohols, promoting the appearance of larger immiscibility domains. The selected fluorinated alcohol was thus 1122- C_8FOH (or 112233- C_9FOH in just one case, for comparison purposes only). Tests with two normal (hydrogenated) alcohols, ethanol and propanol, were

Table 3 Solubility tests in (ionic liquid + fluorinated alcohol) and (ionic liquid + perfluoroalkane) mixtures. M: miscible (one fluid phase system); PM: partially miscible; LPM: low partial miscibility; I: immiscible; LLE: liquid–liquid equilibria; SLE: solid–liquid equilibria. Note that all these fluorinated alcohols are water immiscible. The cells highlighted in bold correspond to systems where the determination of the corresponding fluid phase diagrams was possible

	117-C ₇ FOH	1122-C ₈ FOH	11-C ₈ FOH	112233-C ₉ FOH	11-C ₉ FOH	11-C ₁₀ FOH	C ₇ F ₁₆
P ₆₆₆ 14NTf ₂	M	PM (LLE)	M	—	—	M	I to LPM
P ₆₆₆ 14Cl	M	M	—	—	—	—	I
P ₆₆₆ 14OTf	M	—	M	—	M	M (SLE)	I
P ₆₆₆ 14Ac	—	—	M (SLE)	—	M	foam (LLE)	—
C ₂ mimNTf ₂	M	—	M	—	M	M	—
C ₃ mimNTf ₂	—	PM (LLE)	—	—	—	—	I to LPM
C ₃ mimNTf ₂	M	—	—	—	—	—	I to LPM
C ₈ mimNTf ₂	—	PM (LLE)	—	—	—	—	—
C ₁₀ mimNTf ₂	M	PM (LLE)	M	PM (LLE)	—	M	I to LPM
C ₁₂ mimNTf ₂	M	PM (LLE)	—	—	—	—	I
AcChNTf ₂	—	PM (LLE)	—	—	—	—	—
C ₆ mimCl	—	M	—	—	M	M	—
C ₁₂ mimCl	M	—	—	—	—	—	I
C ₄ mimBF ₄	M	PM (LLE)	M (SLE)	—	—	M (SLE)	—
C ₄ mimPF ₆	M	PM (LLE)	—	—	—	—	I to LPM
C ₈ mimPF ₆	—	PM (LLE)	—	—	—	—	—
C ₁₀ MePy NTf ₂	—	PM (LLE)	—	—	—	—	—
C ₁₂ MePy NTf ₂	—	PM (LLE)	—	—	—	—	—
C ₁₄ MePy NTf ₂	—	PM (LLE)	M	—	—	M	—
C ₁₄ MePy Br	—	PM (LLE)	—	—	—	—	—
ECOENG 212	M	M	M	—	M	gel-like (LLE)	—
AMMOENG 102	—	M	—	—	—	—	I
ALQUAT 336	—	M	M	—	M	M	—
C ₄ mim SCN	—	M	—	—	—	—	—
C ₄ mim SO ₄	—	M	—	—	—	—	—

also performed in order to compare the fluid phase behaviour of their mixtures with ionic liquids.

It should be noted that M. Shiflett and A. Yokozeki^{10,14–16} determined a series of phase diagrams of several small-molecule hydrofluorocarbons with C₂mimNTf₂, C₄mimPF₆, C_nmimBF₄ (*n* = 2 or 4).

The results of the cloud-point determinations are given in Table 4 for the thirteen selected (ionic-liquid + alcohol) systems: ten systems with 1122-C₈FOH (highlighted in Table 3), one system with 1-decyl-3-methylimidazolium bistriflamide plus 112233-C₉FOH, and two with acetylcholinium bistriflamide plus ethanol or propanol.

Fig. 1 (a to d) depicts the fluid phase behaviour of mixtures of dialkylimidazolium bistriflamide ionic liquids with 1122-C₈FOH or 112233-C₉FOH. The figure shows that the fluid phase behaviour is affected by the length of the alkyl side-chains connected to the imidazolium ring of the ionic liquid and by the length of the hydrogenated segment between the perfluorinated chain and the hydroxyl group of the alcohol. It must be stressed that the scale (*x*- and *y*-axes ranges) in Fig. 1 was adjusted to the scale of all subsequent figures that depict the fluid phase behaviour in ionic liquid plus alcohol mixtures (Fig. 3 to 5), in order to facilitate comparisons between them—hence the apparently unused space in panels (a to d) in Fig. 1.

The general trend depicted in Fig. 1 can thus be summarized as follows: (i) ionic liquids with longer alkyl-side chains (in the imidazolium cation) show a larger immiscibility domain with fluorinated alcohols than their shorter-chain counterparts—a behaviour opposite of that shown when *n*-alcohols are mixed with these same ionic liquids,^{17,18} or *N*-alkyl-3-methylpyridinium-

based ionic liquids;¹⁷ (ii) a longer hydrogenated carbon chain—a kind of “spacer”—between the fluorinated chain and the hydroxyl group of the alcohol also decreases the miscibility between the two components of the mixture; and (iii) larger immiscibility regions (an increase in the *T*_{UCST}) are accompanied by a shift in the critical composition to mixtures richer in the fluorinated alcohol.

Trend (i) can be interpreted taking into account the recently discovered nano-structure of ionic liquids, exhibiting high-charge (polar) and low-charge (non-polar) density regions,³ and also their dual nature as they interact with a given solute either *via* the non-polar or polar regions, or (in the latter case) *via* the charged parts of the anion or of the cation.¹ Previous simulation studies,⁵ supported by experimental evidence have shown that the hydroxyl group of alcohols interact strongly with the anions of ionic liquids and also with the hydrogen atoms directly connected to the imidazolium ring (especially the one at C2) and that the alkyl side chain of the alcohol orients itself away from the polar region and towards the non-polar domains of the ionic liquid. To confirm these facts for bistriflamide-based ionic liquids, new Molecular Dynamics simulations were performed within the scope of the present work: methanol and tetrafluoromethane molecules acting as test-solutes and C₄mimNTf₂ acting as the solvent were modelled by explicit-atom force fields.^{19–22} Details of the simulations were similar to those adopted for pure ionic liquids.²³ Due to the slow dynamics of this type of system, special care was taken to ensure that equilibrium conditions were reached, including the proper diffusion of the solutes in the ionic liquid. Equilibration and production runs were implemented for 1 ns and multiple re-equilibrations through the use of temperature annealing

Table 4 Cloud-point temperatures as a function of the ionic liquid mole fraction in different (ionic liquid + alcohol) systems. All systems include the alcohol 1122-C₈FOH, except where stated

x_{IL}	T/K	x_{IL}	T/K	x_{IL}	T/K	x_{IL}	T/K	x_{IL}	T/K	x_{IL}	T/K	x_{IL}	T/K
C ₈ mimNTf ₂		C ₁₂ mimNTf ₂		C ₁₀ MePyNTf ₂		C ₁₄ MePyNTf ₂		AcChNTf ₂ ^b		AcChNTf ₂ ^c		C ₈ mimPF ₆	
0.155	263.9	0.533	282.0	0.575	269.4	0.460	292.1	0.008	308.6	0.268	285.4	0.065	320.0
0.220	266.5	0.060	273.7	0.616	269.0	0.426	292.7	0.017	319.8	0.231	288.1	0.092	323.5
0.302	268.3	0.136	283.2	0.655	266.8	0.378	293.2	0.023	324.7	0.202	290.0	0.115	325.1
0.384	268.3	0.199	284.8	0.694	263.9	0.340	293.5	0.031	328.2	0.179	291.1	0.145	326.0
0.670	264.5	0.739	267.3	0.736	263.0	0.314	293.5	0.041	331.0	0.160	291.8	0.183	327.0
0.569	268.5	0.623	277.2	0.066	259.4	0.270	293.5	0.051	332.5	0.122	292.6	0.232	327.6
0.466	269.2	C ₁₀ mimNTf ₂ ^a		0.097	265.7	0.239	293.4	0.063	333.5	0.088	292.7	0.284	328.1
0.346	268.9	0.093	280.8	0.118	267.8	AcChNTf ₂		0.076	334.1	C ₄ mimBF ₄		P _{6,6,14} NTf ₂	
C ₁₀ mimNTf ₂ ^b		0.118	283.3	C ₁₂ MePyNTf ₂		0.006	282.6	0.093	334.3	0.313	284.3	0.015	283.8
0.038	252.3	0.141	285.5	0.050	267.7	0.017	304.6	0.108	334.4	0.371	287.7	0.021	290.3
0.052	261.2	0.174	287.1	0.083	275.4	0.028	313.6	0.125	334.3	0.404	290.1	0.035	295.9
0.083	267.5	0.222	287.9	0.120	278.5	0.045	319.6	0.153	333.9	0.439	291.9	0.048	300.0
0.102	270.4	0.273	288.3	0.163	281.0	0.064	323.6	0.173	333.4	0.480	294.8	0.063	302.4
0.760	259.9	0.350	287.8	0.200	281.9	0.087	326.1	0.190	332.9	0.508	297.0	0.084	303.6
0.690	266.2	0.406	286.1	0.227	282.7	0.106	327.9	0.181	333.2	0.538	299.1	0.134	305.5
0.625	270.7	0.048	270.3	0.269	283.0	0.129	329.6	0.212	331.8	0.572	301.2	0.180	306.1
0.045	256.9	0.072	276.6	0.331	283.1	0.169	330.7	0.248	329.5	0.601	302.8	0.234	306.1
0.067	262.9	0.062	274.3	0.418	282.5	0.202	331.4	0.289	326.4	0.621	303.7	0.381	303.2
0.080	266.0	0.078	278.1	0.638	273.6	0.227	331.8	0.629	275.7	0.609	303.5	0.445	300.7
0.094	268.6	0.291	288.2	0.560	278.0	0.255	332.0	0.553	292.3	0.645	304.8	0.518	295.8
0.121	270.8	0.329	288.0	0.508	281.0	0.286	332.3	0.422	311.5	0.696	306.5	0.634	284.3
0.139	272.2	0.388	286.6	C ₁₄ MePyNTf ₂		0.318	332.2	0.340	321.4	0.744	307.8	0.686	278.2
0.168	274.1	0.451	284.9	0.020	267.2	0.348	332.4	0.242	329.8	0.805	308.7	0.013	280.9
0.185	274.4	0.501	283.0	0.034	277.5	0.374	332.0	AcChNTf ₂ ^c		0.846	309.4	0.028	293.6
0.219	275.0	0.573	279.3	0.045	281.2	0.412	332.0	0.009	255.3	0.986	301.3	0.058	301.7
0.261	275.6	0.648	273.0	0.066	286.7	0.311	332.8	0.011	258.4	0.942	307.5	0.085	303.9
0.313	276.0	0.703	269.3	0.082	288.5	0.394	332.4	0.014	273.4	0.794	307.1	0.114	305.3
0.260	275.9	C ₁₀ MePyNTf ₂		0.106	290.7	0.456	332.2	0.018	275.5	0.818	307.1	0.163	306.0
0.329	276.1	0.111	266.8	0.126	291.7	0.519	331.2	0.019	276.5	0.851	307.3	0.215	306.0
0.382	275.8	0.146	271.0	0.153	292.6	0.559	330.5	0.024	283.8	0.890	306.4	0.268	305.8
0.436	275.6	0.183	273.0	0.191	293.1	0.594	329.9	0.027	285.5	0.982	296.1	0.315	304.8
0.480	274.1	0.220	273.7	0.222	293.2	0.630	328.8	0.030	286.8	0.959	303.0	0.770	263.3
0.527	273.1	0.278	274.5	0.820	263.5	0.671	326.8	0.034	288.3	0.924	304.9	0.568	292.0
0.565	272.2	0.313	274.6	0.768	271.1	0.712	323.4	0.041	289.7	0.691	304.2		
0.605	270.6	0.349	274.0	0.705	278.1	0.749	320.4	0.072	292.2	0.479	294.2		
0.653	268.3	0.386	273.9	0.647	283.6	0.910	280.4	0.104	292.8	0.591	300.5		
0.730	263.0	0.424	273.0	0.610	286.2	0.853	302.5	0.143	292.2	0.405	293.2		
C ₁₂ mimNTf ₂ ^c		0.438	273.6	0.569	288.4	0.801	314.5	0.520	251.6	0.645	306.6		
0.273	285.8	0.483	273.0	0.528	290.0	0.831	308.8	0.400	269.8	C ₈ mimPF ₆			
0.393	285.2	0.529	272.2	0.493	291.2	0.722	322.8	0.325	279.4	0.041	314.3		

^a 112233-C₉FOH. ^b Propanol. ^c Ethanol.

and/or switching off and on of the Coulomb interactions were performed. The temperature, pressure and low concentration of the solutions ensured that they were performed in the one-phase region of each system. Solvent–solute radial distribution functions (RDFs) for selected atoms from each species (solute, cation and anion) were calculated from the structural simulation data and are shown in Fig. 2. Fig. 2a describes the position of the hydroxyl hydrogen atom of methanol (HO) relative to different atoms of the ionic liquid. The strong interaction of HO with the oxygen atom of bistriflamide (OBT) is obvious and confirms the statements produced at the beginning of this paragraph. On the other hand, the RDFs of Fig. 2b show how the methanol molecule orients itself in relation to the strong interaction centre OBT: the succession of the three peaks clearly shows that the hydrogen points towards the oxygen atom (possibly forming an hydrogen bond), while the methyl group points in the opposite direction (towards the less polar regions of the ionic liquid, *cf.* below). Finally, Fig. 2c shows the RDFs describing the position of the carbon atom of CF₄ (CFC) relative to different atoms of

the anion or cation of the ionic liquid. The changes are dramatic in relation to Fig. 2a: the solute is now positioned in the non-polar domains of the ionic liquid, as denoted by the RDF of CFC with the end-carbon of the butyl group of the cation, CT. However the different RDFs also show that there is a certain degree of affinity between CFC and the fluorine atoms of the CF₃ groups of bistriflamide (*cf.* the CFC–FBT radial distribution function), which means that probably the perfluorinated solutes will prefer to stay away from the polar regions of the ionic liquid but as close as possible to the CF₃ groups of bistriflamide. We must keep in mind that the interactions of perfluorocarbons with hydrocarbons are quite unfavourable and in this particular case the position of the perfluorinated solute is dictated simply by the less unfavourable position, a situation that can be partially mitigated by some (favourable) interactions with other (not so dissimilar) CF₃ groups.

Returning to the discussion of the systems studied experimentally, in the case of the fluorinated alcohols with an ethyl or propyl “spacer” group, 1122-C₈FOH or 112233-C₉FOH,

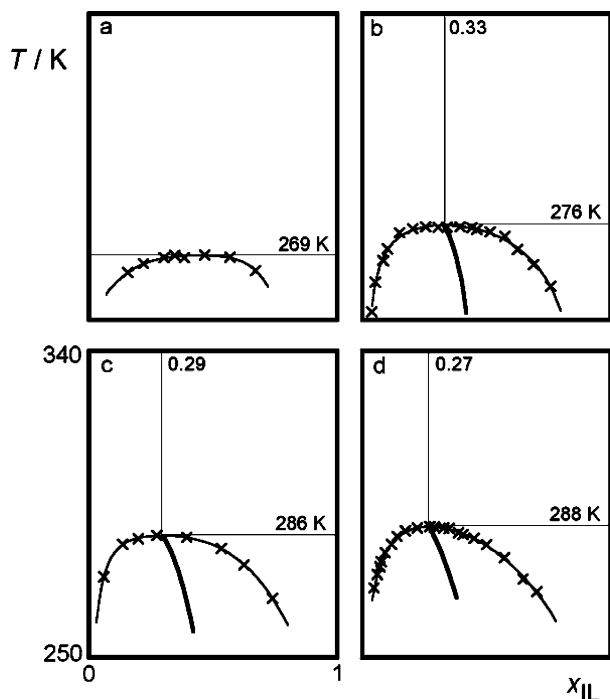


Fig. 1 Cloud-point temperature, T , as a function of composition (mole fraction of ionic liquid, x_{IL}) in (a) $\text{C}_8\text{mimNTf}_2 + 1122\text{-C}_8\text{FOH}$; (b) $\text{C}_{10}\text{mimNTf}_2 + 1122\text{-C}_8\text{FOH}$; (c) $\text{C}_{12}\text{mimNTf}_2 + 1122\text{-C}_8\text{FOH}$; and (d) $\text{C}_{10}\text{mimNTf}_2 + 112233\text{-C}_9\text{FOH}$. (x): experimental cloud-point data; black lines represent fittings to each side of the liquid–liquid equilibrium envelope; grey lines represent the average composition as determined by the rectilinear diameter law. Also shown are the estimated values for the upper critical solution temperature, T_{UCST} , and critical composition.

respectively, the perfluorinated segment will be thrown by the hydrogenated segment deep into the non-polar region of the ionic liquid, where the interactions are unfavourable and the driving force towards phase separation is larger. When the alkyl side-chains of the cation are longer, the nano-segregation is more noticeable and the non-polar domains are larger, which means that the immiscibility regions will also increase, as can be observed in the series of mixtures depicted in Fig. 1a to 1c.

Trend (ii) is noticeable not only by the comparison between Fig. 1b and 1d—a T_{UCST} upwards shift of ~ 12 K—but also by the fact that fluorinated alcohols with just one hydrogenated atom of carbon exhibit complete miscibility with the ionic liquid (*cf.* Table 3). Conversely, perfluorinated alkanes—with no spacer and no hydroxyl group—exhibit large immiscibility walls (complete immiscibility or very limited partial miscibility, *cf.* last column of Table 3) with different ionic liquids.²⁴ This trend can also be interpreted by the “dual-nature” arguments presented in the previous paragraphs. In fact, the increased miscibility of perfluorinated alcohols or fluorinated alcohols with short spacers (such as methyl) can be better understood if one also recognizes the presence of “fluorinated-friendly” residues included in (or adjacent to) the polar domains of the ionic liquid: the perfluoromethyl groups present at the ends of the bistriflamide anion. In the case of fluorinated alcohols with no or short spacers, the hydroxyl group will anchor the alcohol “head” near the polar regions and the short spacer will allow the perfluorinated chain to remain close to the polar domain

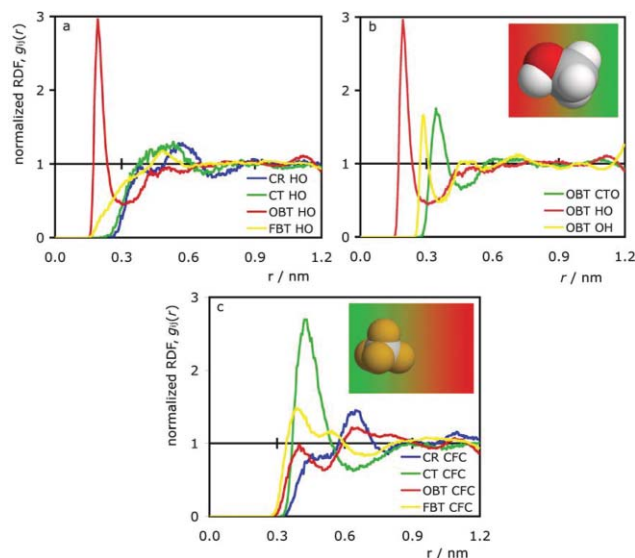


Fig. 2 Solute–solvent radial distribution functions showing the position and orientation of methanol (a and b) and tetrafluoromethane (c) dissolved in $[\text{C}_4\text{mim}][\text{NTF}_2]$. The insets indicate schematically the preference of each solute for the high-charge (red) or low-charge (green) regions of the ionic liquid. HO, OH and CTO represent the hydrogen (hydroxyl), oxygen and carbon atoms of methanol, respectively; CR the carbon atom between the two nitrogens of the imidazolium ring; CT the terminal carbon in the butyl chain of the cation; and OBT and FBT the oxygen and fluorine atoms of the anion, respectively. CFC holds for the carbon atom of tetrafluoromethane.

where it can orient itself towards the end groups of bistriflamide, thus increasing the mutual miscibility of the alcohol and the ionic liquid. When the hydroxyl group is absent (as in the case of perfluoroalkanes) no anchoring process is possible and the perfluorinated compound (that has no driving force to stay close to the polar regions) will exhibit large immiscibility windows in mixtures with ionic liquids.

Trend (iii) will be discussed below, when other ionic liquids and alcohols with different volume ratios are presented.

In Fig. 3 mixtures with a different family of ionic liquids—*N*-alkyl-3-methylpyridinium bistriflamide—are shown. The only difference between the previous systems and the present ones is the “head” of the cation that was “switched” from a methyl-imidazolium ring to a methyl-pyridinium one (*cf.* Table 1).

The differences between Fig. 1 and 3, especially when ionic liquids with the same alkyl side-chain length are compared (Fig. 1b and 3a; Fig. 1c and 3b), are very small both in terms of the upper critical solution temperatures and concentrations. This lends support to the view that no specific interactions between the fluorinated alcohol and the charged part of these two particular ionic liquid cations are present in the mixture. The structural similarity between the two head groups of the cations (both alkyl-substituted hetero-aromatic rings) also explains the similarity of the fluid phase behaviour.

The acetylcholinium cation was tested in the systems represented in Fig. 4. The most obvious difference in relation to the systems presented in Fig. 1 and 3 is that by changing the structural nature of the cation (the long alkyl side chain was changed into a shorter, functionalized one; the hetero-aromatic head group was replaced by a tetra-alkyl ammonium cation)

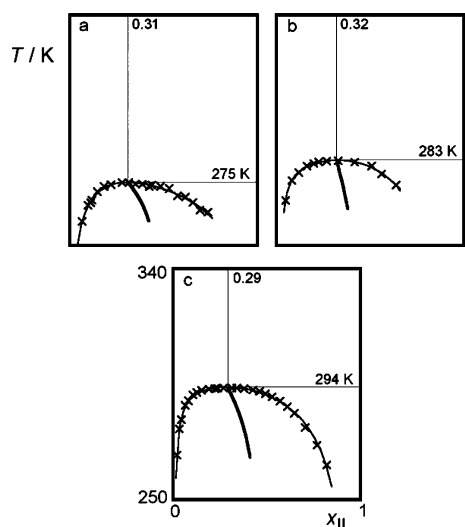


Fig. 3 Cloud-point temperature as a function of composition (mole fraction of ionic liquid) in (a) $C_{10}MePyNTf_2 + 1122-C_8FOH$; (b) $C_{12}MePyNTf_2 + 1122-C_8FOH$; and (c) $C_{14}MePyNTf_2 + 1122-C_8FOH$. Symbols and lines as in Fig. 1.

the immiscibility window with the fluorinated alcohol increases dramatically.

It is hard to interpret these results in terms of the polar/non-polar structure of the ionic liquid and of the specific interactions of the fluorinated alcohol with the anion. In acetylcholinium-based ionic liquids one can argue that the functionalization of the alkyl side-chain with an ester group increases the charge density of the non-polar regions, eventually reducing the segregated character of the ionic liquid and decreasing the size of its non-polar domains. This can be discussed in terms of the results presented in Fig. 4b, where the solubility of ethanol and propanol in $AcChNTf_2$ is shown. At room temperature (298 K) ethanol is completely miscible with $AcChNTf_2$, exhibiting an upper critical solution temperature at around 293 K. The corresponding value for the propanol mixtures is 338 K, signalling a much larger immiscibility domain. This can be easily understood in terms of the inability of the ionic liquid to accommodate the longer alkyl moieties of the propanol among its functionalized, high charge-density, alkyl side-chains. However, the increased immiscibility of the fluorinated alcohol in $AcChNTf_2$ cannot be understood considering only the partial destruction of the non-polar regions of the latter substance. In fact, we saw in previous systems that a smaller non-bonded region increased

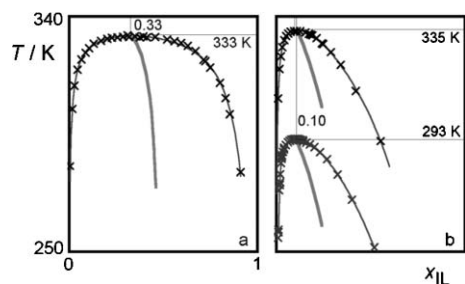


Fig. 4 Cloud-point temperature as a function of composition (mole fraction of ionic liquid) in (a) $AcChNTf_2 + 1122-C_8FOH$; (b) $AcChNTf_2 + C_3H_8OH$ (top); $AcChNTf_2 + C_2H_5OH$ (bottom). Symbols and lines as in Fig. 1.

the miscibility. The detail that is missing is that now the hydroxy group of the fluorinated alcohol can interact not only with the oxygen atoms of bistriflamide (and orient its fluorinated moiety towards the CF_3 end-groups of that anion) but also interact with the oxygen atoms of the ester group (which implies the presence of the fluorinated residue in the midst of the alkyl side chain of the cation). This competition will promote the immiscibility of the fluorinated alcohol in the acetylcholinium-based ionic liquid.

Fig. 5 presents the results for mixtures of different types of ionic liquid with the fluorinated alcohol 1122- C_8FOH . In this case both the cation and the anion were changed.

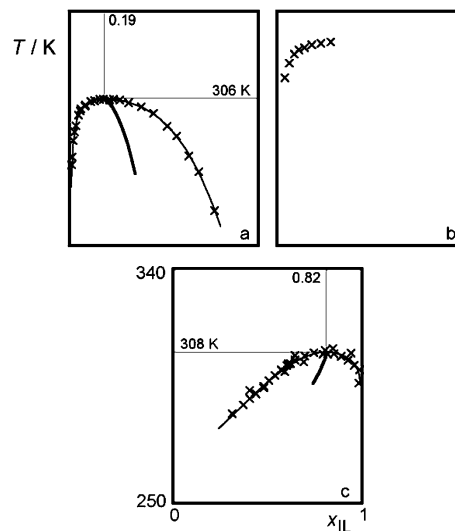


Fig. 5 Cloud-point temperature as a function of composition (mole fraction of ionic liquid) in (a) $P_{6614}NTf_2 + 1122-C_8FOH$; (b) $C_8mimPF_6 + 1122-C_8FOH$; (c) $C_4mimBF_4 + 1122-C_8FOH$. Symbols and lines as in Fig. 1.

In Fig. 5a we show the fluid phase diagram of mixtures of the fluorinated alcohol with a tetra-alkylphosphonium-based ionic liquid with bistriflamide as counter-ion. The immiscibility envelope lies somewhere in between those of imidazolium- and pyridinium-based ionic liquids (Fig. 1 and 3) and that of the acetylcholinium-based ionic liquid (Fig. 4a). Immiscibility is larger than in the former cases because the non-polar regions are bigger (four alkyl side-chains) and surround the charged part of the ionic liquid (the phosphorus atom in the cation and the bistriflamide anion), making it more difficult for the alcohol to anchor and orient itself favourably in the vicinity of the anion. On the other hand, miscibility is larger than in the acetylcholinium case due to the absence of the ester groups in the alkyl-side chains (*cf.* discussion above).

In Fig. 5b, the bistriflamide anion of the ionic liquid was substituted by the hexafluorophosphate anion. The fluid phase diagram is incomplete due to decomposition problems at the temperatures that needed to be attained to measure the corresponding cloud-points (one of the reasons behind the increasing popularity of bistriflamide as the “standard” anion in many recent studies involving ionic liquids is its enhanced thermal stability relative to other anions such as PF_6 or BF_4). Nevertheless, it is possible to conclude that the immiscibility is quite high, probably due to the size and rigidity of the anion

that while interacting with the hydroxyl group of the fluorinated alcohol does not allow at the same time the interaction of the fluorinated residue of the latter with the fluorinated atoms of the former.

In Fig. 5c, we tested a tetrafluoroborate anion-based ionic liquid. In order to decrease the working temperatures and avoid decomposition problems we decided to use an imidazolium cation with a shorter alkyl side-chain (as we saw in previous cases, smaller non-polar domains in the ionic liquid increase the solubility of the fluorinated alcohol). The fluid phase diagram of the mixture still exhibits a relatively high upper critical solution temperature (higher than the corresponding bistriflamide imidazolium-based ionic liquid of Fig. 1) for the same reasons pointed out in the previous paragraph.

However, the most interesting feature of the diagram in Fig. 5c is the shift to higher ionic liquid mole fraction of the upper critical solution concentration. Part of the shift can be attributed to the difference in size between the components of the mixture: components with similar size generally exhibit symmetrical $T-x$ immiscibility windows centred at the equimolar concentration, whereas mixtures with components very dissimilar in size will have the LLE envelope leaning towards the smaller component. This can explain trend (iii) observed in Fig. 1 (see above): as the alkyl side-chain of the ionic liquid is increased (its volume is larger) the diagrams shift to the side of the alcohol (lower ionic liquid mole fraction) and the corresponding critical concentration is decreased. The same applies to Fig. 4: when the fluorinated alcohol is substituted by (the much smaller) ethanol or propanol molecules, the corresponding diagrams and critical concentrations also shift (markedly) to more alcohol-rich compositions. In this case, we have the smallest of all studied ionic liquids, which means that we would anticipate a shift of the critical concentration to the ionic-liquid-rich side of the diagram. That is indeed the case, but the surprise is the magnitude of the shift: the molar volumes of the fluorinated alcohol and of C_4mimBF_4 are quite similar (216.7 and 187.6 $\text{cm}^3 \text{mol}^{-1}$, respectively, *cf.* Table 5), which would indicate a critical concentration close to the equimolar, not $x_{iL} = 0.82$.

Lattice models like the modified Flory–Huggins, FH, theory proved to be valuable tools to interpret liquid–liquid equilibrium behaviour, namely the prediction of the locus of the critical solution concentration in binary mixtures containing ionic liquids.³¹ According to those models, the critical solution concentration, expressed in mole fraction of component 1, can be expressed as $x_{1,c} = 1/(1 + r^{3/2})$, where r is the ratio between the molar volume of the components, $r = V_{m,1}/V_{m,2}$. The aforementioned relation was applied to the systems studied in this work and it was found (*cf.* Table 5) that the relation yields good results for all of them except for the $C_4mimBF_4 + 1122-C_8FOH$ mixtures. This fact suggests that there is some degree of association between the fluorinated molecules in the one-phase region above the UCST—the mixture is not completely random. For instance, if we consider that, on average, the fluorinated alcohol molecules form dimers (with a volume twice that of the isolated molecules) than the corresponding value of $x_{1,c}$ would rise from the 0.544 value presented in Table 5 to a value of 0.778, in better agreement with the experimental value. Such self-aggregation (possibly through the fluorinated “tails” of the alcohol) would compensate for the possible loss of F–F interactions when the anion of the ionic liquid is changed from bistriflamide to tetrafluoroborate and would explain the sudden change in the shape of the liquid–liquid immiscibility envelope in Fig. 5c.

The effect of pressure on the liquid–liquid immiscibility window of selected ionic liquid plus partially fluorinated alcohol was also investigated. The shift of the cloud point temperature as a function of pressure for four mixtures containing 1122- C_8FOH and $C_8mimNTf_2$, $C_{10}mimNTf_2$, $C_{12}mimNTf_2$, or $C_{12}MePyNTf_2$, each at their corresponding critical composition (*cf.* Fig. 1a–1c and 3b), is presented in Fig. 6. The graph shows that in these systems the cloud-point temperatures are almost not affected by pressure—less than 0.2 K per MPa increase in all cases (see caption to figure).

The fact that these slopes, dT/dp , are positive imply that the mixing process at temperatures near and above the UCST in these systems (fluorinated alcohols + bistriflamide- and imidazolium-based or pyridinium-based ionic liquids) is accompanied by a volume expansion (positive excess volume,

Table 5 Critical solution concentration (estimated, FH, and experimental, exp) in different (ionic liquid(1) + alcohol(2)) systems. All systems include the alcohol 1122- C_8FOH , except where stated. The molar volume of each component at 298 K is also given. Numbers as superscripts hold for references

	$C_8mimNTf_2$	$C_{10}mimNTf_2$	$C_{12}mimNTf_2$	$C_{10}MePyNTf_2$	$C_{12}MePyNTf_2$	$C_{14}MePyNTf_2$
$V_{m1}/\text{cm}^3 \text{mol}^{-1}$	362.1 ²⁵	404.1 ²⁵	429.8 ^{1,26,e}	407.6 ²⁷	440.1 ²⁷	473.2 ²⁷
$V_{m2}/\text{cm}^3 \text{mol}^{-1}$	216.4 ^d	216.4 ^d	216.4 ^d	216.4 ^d	216.4 ^d	216.4 ^d
$x_{1,c}$ (FH)	0.317	0.283	0.264	0.279	0.257	0.237
$x_{1,c}$ (exp)	0.47	0.330	0.294	0.309	0.323	0.291
	$C_{10}mimNTf_2^a$	$AcChNTf_2$	$AcChNTf_2^b$	$AcChNTf_2^c$	$P_{6,6,14}NTf_2$	C_4mimBF_4
$V_{m1}/\text{cm}^3 \text{mol}^{-1}$	404.1 ²⁵	287.4 ²⁸	287.4 ²⁸	287.4 ²⁸	716.3 ²⁶	187.6 ²⁹
$V_{m2}/\text{cm}^3 \text{mol}^{-1}$	234.2 ^d	216.4 ^d	75.2 ³⁰	58.7 ³⁰	216.4 ^d	216.4 ^d
$x_{1,c}$ (FH)	0.304	0.396	0.118	0.084	0.143	0.554
$x_{1,c}$ (exp)	0.269	0.334	0.109	0.101	0.186	0.815

All systems include the alcohol 1122- C_8FOH , except^a 112233- C_9FOH . ^b Propanol. ^c Ethanol. ^d Density measured in the present work using an Anton-Paar DMA 5000 vibrating-tube densimeter. ^e Molar volume estimated as the sum of the effective volumes occupied by the cation and anion (see ref. 1,26).

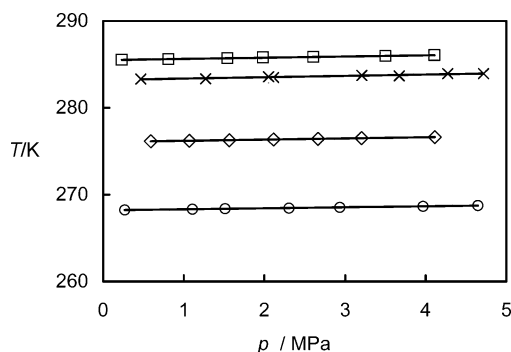


Fig. 6 Pressure dependence of cloud-point temperature in partially fluorinated alcohol plus ionic liquid systems near their critical composition. Values for the slope in mK/MPa are given between parentheses for each system. (□) 1122-C₈FOH + C₈mimNTf₂ (118); (◇) 1122-C₈FOH + C₁₀mimNTf₂ (140); (○) 1122-C₈FOH + C₁₂mimNTf₂ (138); (×) 1122-C₈FOH + C₁₂MePyNTf₂ (158).

$\Delta V^E > 0$). The rationale for this fact is found at the recently revisited^{32,33} Prigogine–Defay relation, which states that under some restrictive assumptions (in practice, the two excess properties, ΔV^E and ΔH^E , have to have a similar form in respect to composition and present no inflection points), one obtains a Clapeyron-type of relation, which can be expressed as:

$$\left(\frac{dT}{dp}\right)_c \cong T_c(p) \frac{\Delta V^E(T_c(p), x)}{\Delta H^E(T_c(p), x)} \quad (1)$$

Then, one should recognize that demixing upon cooling (UCST-type of phase diagram) is an exothermic process, thus, conversely, mixing is endothermic ($\Delta H^E > 0$).

4. Conclusions

In this work, liquid–liquid equilibria (cloud-point temperature determinations) of binary mixtures of fluorinated alcohols plus different ionic liquids were studied and measured by turbidimetry. These systems comprise two classes of fluids that, due to their unique characteristics, are very interesting both from the pure and applied chemistry points of view and have, in recent years, received increasing attention from the scientific community.

The corresponding T – x phase diagrams exhibit a rich fluid-phase behaviour that can be rationalized semi-quantitatively at the molecular level in terms of the different and complex interactions between the fluorinated alcohol—composed of a polar head group, an alkylated “spacer”, and a fluorinated moiety—and the ionic liquid—a micro-segregated fluid exhibiting non-polar domains permeated by a polar network.

The possibility of using fluorinated alcohols (or other diblock molecules with fluorinated residues) together with bistriflamide-based ionic liquids in order to promote the miscibility of the latter with water (and water-soluble molecules) is one of the potential future developments of the present work.

Acknowledgements

This work was supported by the *Fundação para a Ciência e Tecnologia (FC & T)*, Portugal (POCI/QUI/57716/2004 and PTDC/CTM/73850/2006). M. B. thanks *FC & T* for a Ph.D.

grant SFRH/BD/13763/2003. We would like to thank the QUILL team, Belfast, for the synthesis and characterization of several ionic liquids used in this work.

References

- 1 L. P. N. Rebelo, J. N. Canongia Lopes, J. M. S. S. Esperança, J. Lachwa, V. Najdanovic-Visak and Z. P. Visak, *Acc. Chem. Res.*, 2007, **40**, 1114–1121.
- 2 N. V. Plechkova and K. R. Seddon, *Chem. Soc. Rev.*, 2008, **37**, 123–150.
- 3 J. N. Canongia Lopes and A. A. H. Pádua, *J. Phys. Chem. B*, 2006, **110**, 3330–3335.
- 4 M. S. Kelkar and E. J. Maginn, *J. Chem. Phys.*, 2005, **123**.
- 5 J. N. Canongia Lopes, M. F. Costa Gomes and A. A. H. Pádua, *J. Phys. Chem. B*, 2006, **110**, 16816–16818.
- 6 R. E. Banks, B. E. Smart, J. C. Tatlow, *Organofluorine Chemistry – Principles and Commercial Applications*, Plenum Press, New York, 1994.
- 7 J. G. Riess, *Chem. Rev.*, 2001, **101**, 2797–2919.
- 8 C. A. Eckert, B. L. Knutson and P. G. Debenedetti, *Nature*, 1996, **383**, 313–318.
- 9 M. J. P. de Melo, A. M. A. Dias, M. Blesic, L. P. N. Rebelo, L. F. Vega, J. A. P. Coutinho and I. M. Marrucho, *Fluid Phase Equilib.*, 2006, **242**, 210–219.
- 10 M. B. Shiflett and A. Yokozeki, *Ind. Eng. Chem. Res.*, 2008, **47**, 926–934.
- 11 P. Morgado, H. G. Zhao, F. J. Blas, C. McCabe, L. P. N. Rebelo and E. J. M. Filipe, *J. Phys. Chem. B*, 2007, **111**, 2856–2863.
- 12 J. R. Trindade, A. M. A. Dias, M. Blesic, N. Pedrosa, L. P. N. Rebelo, L. F. Vega, J. A. P. Coutinho and I. M. Marrucho, *Fluid Phase Equilib.*, 2007, **251**, 33–40.
- 13 H. C. de Sousa and L. P. N. Rebelo, *J. Chem. Thermodyn.*, 2000, **32**, 355–387.
- 14 M. B. Shiflett and A. Yokozeki, *J. Chem. Eng. Data*, 2008, **53**, 492–497.
- 15 M. B. Shiflett and A. Yokozeki, *Fluid Phase Equilib.*, 2007, **259**, 210–217.
- 16 M. B. Shiflett and A. Yokozeki, *J. Chem. Eng. Data*, 2007, **52**, 2413–2418.
- 17 J. M. Crosthwaite, M. J. Muldoon, S. Aki, E. J. Maginn and J. F. Brennecke, *J. Phys. Chem. B*, 2006, **110**, 9354–9361.
- 18 J. M. Crosthwaite, S. Aki, E. J. Maginn and J. F. Brennecke, *J. Phys. Chem. B*, 2004, **108**, 5113–5119.
- 19 W. L. Jorgensen, D. S. Maxwell and J. TiradoRives, *J. Am. Chem. Soc.*, 1996, **118**, 11225–11236.
- 20 E. K. Watkins and W. L. Jorgensen, *J. Phys. Chem. A*, 2001, **105**, 4118–4125.
- 21 J. N. C. Lopes, J. Deschamps and A. A. H. Padua, *J. Phys. Chem. B*, 2004, **108**, 11250.
- 22 J. N. C. Lopes, J. Deschamps and A. A. H. Padua, *J. Phys. Chem. B*, 2004, **108**, 2038–2047.
- 23 J. Lopes and A. A. H. Padua, *J. Phys. Chem. B*, 2006, **110**, 3330–3335.
- 24 T. L. Merrigan, E. D. Bates, S. C. Dorman and J. H. Davis, *Chem. Commun.*, 2000, 2051–2052.
- 25 J. N. C. Lopes, T. C. Cordeiro, J. Esperanca, H. J. R. Guedes, S. Huq, L. P. N. Rebelo and K. R. Seddon, *J. Phys. Chem. B*, 2005, **109**, 3519–3525.
- 26 J. Esperanca, H. J. R. Guedes, M. Blesic and L. P. N. Rebelo, *J. Chem. Eng. Data*, 2006, **51**, 237–242.
- 27 P. Natalia, *PhD Thesis*, Queens University of Belfast, 2007.
- 28 G. W. Driver, *PhD Thesis*, Queens University of Belfast, 2007.
- 29 R. G. de Azevedo, J. Esperanca, V. Najdanovic-Visak, Z. P. Visak, H. J. R. Guedes, M. N. da Ponte and L. P. N. Rebelo, *J. Chem. Eng. Data*, 2005, **50**, 997–1008.
- 30 G. C. Benson and H. D. Pflug, *J. Chem. Eng. Data*, 1970, **15**, 382.
- 31 V. Najdanovic-Visak, J. Esperanca, L. P. N. Rebelo, M. N. da Ponte, H. J. R. Guedes, K. R. Seddon, H. C. de Sousa and J. Szydowski, *J. Phys. Chem. B*, 2003, **107**, 12797–12807.
- 32 L. P. N. Rebelo, *Phys. Chem. Chem. Phys.*, 1999, **1**, 4277–4286.
- 33 H. C. De Sousa and L. P. N. Rebelo, *J. Polym. Sci., Part B: Polym. Phys.*, 2000, **38**, 632–651.